The Effect of Rate Design on Power Distribution Reliability Considering Adoption of Distributed Energy Resources

Aditya Maheshwari^a, Miguel Heleno^{b,*}, Michael Ludkovski^a

^a University of California, Santa Barbara, CA, USA ^b Lawrence Berkeley National Laboratory, Berkeley, CA, USA

Abstract

Electricity rates are a main driver for adoption of Distributed Energy Resources (DERs) by private consumers. In turn, DERs are a major component of the reliability of energy access in the long run. Defining reliability indices in a paradigm where energy is generated both behind and in front of the meter is part of an ongoing discussion about the future role of utilities and system operators with many regulatory implications. This paper contributes to that discussion by analyzing the effect of rate design on the long term reliability indices of power distribution. A methodology to quantify this effect is proposed and a case study involving photovoltaic (PV) and storage technology adoption in California is presented. Several numerical simulations illustrate how electricity rates affect the grid reliability by altering dispatch and adoption of the DERs. We further document that the impact of rate design on reliability can be very different from the perspective of the utility versus that of the consumers. Our model affirms the positive connection between investments in DERs and the grid reliability and provides an additional tool to policy-makers for improving the reliability of the grid in the long term.

Keywords: DER Planning, Rate Design, Reliability, Microgrids.

Nomenclature

Parameters

 Ann_k Ann. interest rate for investments in tech. k

CEff Charging efficiency of the battery

 $CFix_k$ Fixed cost of technology k (\$)

 $CVar_k$ Variable cost of technology k ($kW or \kwh)$

DEff Discharging efficiency of the battery

*Corresponding author

Email address: miguelheleno@lbl.gov (Miguel Heleno)

- EC_t Energy cost at time t (\$)
- FI_t Feed-in remuneration at time t (\$)
- Ld_t Consumer load at time t (kW)
- MiSoc Minimum battery state-of-charge ([0, 1])
- OMV_k O&M costs of technology k (\$/kW or \$/kWh)
- PCr Battery maximum power/capacity ratio
- SR_t Normalized solar gen. at t (kWh/kW installed)

Sets

- \mathcal{I}_t Set of consumers connected to utility at time t
- \mathcal{T} $\mathcal{T}_{yr} \bigcup \mathcal{T}_{fr}$
- \mathcal{T}_{fr} Set of failure-repair times
- \mathcal{T}_{yr} Set of hourly time points over a year
- k Technology type (PV, Storage)
- t Time (hr) in \mathcal{T}_{yr}

Variables

- α Charging/discharging aux. variable (binary)
- cap_k Installed capacity of technology k (kW/kWh)
- ch_t Battery charge at time t (kW)
- dch_t Battery discharge at time t (kW)
- i_k Investment decision for tech. k (binary)
- pv_t PV output at time t (kW)
- soc_t Battery state of charge at time t (kWh)
- ue_t Electricity export to utility at time t (kW)
- ui_t Import from utility at time t (kW)

1. Introduction

To achieve emission targets, countries need to increase generation share from renewable energy sources, not only as part of the bulk generation system but also at the level of the distribution grid [1], where private owned photovoltaic (PV) systems – installed behind the meter and coupled with electric storage and control technologies – have been seen as an efficient way to increase decentralized renewables penetration. Ambitious policy targets have been announced to promote adoption of these Distributed Energy Resources (DERs) by private consumers, such as the new amendment to the Building Energy Efficiency standard in California that requires new residential buildings to have a rooftop PV unit installed starting in 2020 [2]. Such policy measures will continue driving down the cost of solar panels and related technologies, such as storage, creating conditions for a massive adoption.

Besides the technology costs, mass adoption of PV and storage by private consumers is also dependent on the portfolio of electricity tariffs offered by utilities. In fact, the magnitude and structure of tariffs – including demand charges, energy rates and PV feed-in remuneration – strongly affect the payback period of these investments, acting as a second main driver for adoption [3, 4, 5, 6]. Mechanisms of rate design to promote consumers' adoption of DERs are presented in [3] and [4]. In case of PV adoption, the authors of [5] identify feed-in tariffs as a main socio-economic component for adoption; in [6] the dynamics between retail electricity rates and PV adoption are evaluated.

While not the primary reason for the deployment of DERs, distribution grid security and reliability is also impacted by the presence of DERs, see e.g. [7] and [8]. Recent studies have explored the use of utility owned DERs to manage outages and improve the reliability of distribution systems, especially when these DERs comprise dispatchable technologies, such as battery storage [9], electric vehicles (EV) [10, 11] and demand response (DR) [12, 13], or when located in active portions of the distribution system, e.g. microgrids [14]. In contrast, DERs placed behind the meter are outside of utilities' jurisdiction and therefore can only be indirectly influenced by price signals (e.g. tariffs) to support grid operation [15, 16, 17]. For example, energy [15] and power [16] based dynamic tariffs can be used to indirectly change the dispatch of EVs in order to alleviate congestion. Similarly, time-differentiated energy prices can be offered to incentivize DR behaviours that impact the reliability of the distribution grid [17]. In fact, as shown in [17], time-varying tariffs can produce changes in consumers net load that significantly affect the magnitude and time distribution of reliability indices, such as energy not supplied.

These contributions regarding dynamic tariffs applied to EVs and DR together with the extensive literature on time-of-use (ToU) and peak demand rates demonstrate the effectiveness of tariffs in changing consumption behaviors and, more recently, in indirectly "dispatching" DERs in order to solve medium- and short-term operational challenges of distribution systems. However, as pointed above, the effect of tariffs goes beyond the operational time scale and rate design can be used to indirectly drive long-term adoption of DERs by private consumers. Thus, tariffs could be included in the utility planning process to create favourable scenarios of DER deployment from the reliability perspective.

This paper presents a methodology to quantify the impact of electricity tariffs on the long-term reliability of distribution systems, considering dynamic (tariff-dependent) adoption of DERs by private consumers. This adds another layer of complexity to the reliability analysis performed in [17], by capturing the effect of tariff design both on short-term (dispatch) and long-term (adoption) time scales. To the best of the authors' knowledge, such methodology does not exist in the literature. It is essential to the ongoing discussion on the new paradigm of rate design in distributed networks with high penetration of DERs [3, 4, 18, 19]. We use the proposed methodology to analyze the effect of different aspects of the magnitude and structure of electricity tariffs on the average energy not supplied (AENS) from the utility, as well as on the actual magnitude and duration of outages experienced by the consumers. In particular, we are able to quantify the positive link between DER behind-the-meter adoption and grid reliability. A case study involving a PG&E 69 node feeder, where consumers adopt PV and storage technologies, is used to illustrate the approach.

The paper is organized as follows: Section 2 presents the adoption model; Section 3 describes the Monte Carlo simulation of system states and the storage model during line failures applied to compute the reliability indices; Section 4 provides a case study where the reliability impact of different aspects of tariff design is evaluated; finally, Section 5 presents the main conclusions.

2. Adoption Model

In this section, we model adoption of behind-the-meter DERs by private consumers, assuming economic rationality in long-term consumers' decisions related to the acquisition and utilization of DER technologies. This economic rationality is presented as an optimization model, where individual consumers size and dispatch their DER assets in ways that minimize their energy costs. It is important to stress that this approach differs from more complete socioeconomic models of adoption and diffusion that usually capture short-term social and geographical aspects of consumers' decisions, such as the ones used in [5] and [20]. However those models require detailed characterization of specific regions and consumer groups and do not allow general conclusions. Thus, in the context of long-term evaluation of adoption, and with the purpose of deriving general conclusions (not socioeconomic/spatial dependent), we assume economic rationality as the single criterion for adoption. The approach used in this paper is part of the Distributed Resources Customer Adoption Model (DER-CAM), a DER adoption and microgrid planning tool developed by Lawrence Berkeley National Laboratory. For a detailed explanation about the background knowledge and research used to build the adoption model presented below, we refer to the methods related to the PV and storage in [21].

The objective function minimizes the fixed/variable costs for investments in DERs (in this paper we consider only PV and storage). The cost function also takes into account the tariffs, i.e. the hourly costs of energy and the remuneration paid by the utility for the energy injected into the grid. The cost function is

given as:

$$c = \sum_{k \in \{s, pv\}} \left(CFix_k \cdot i_k + CVar_k \cdot cap_k \right) Ann_k + \sum_{t \in \mathcal{T}_{yr}} (ui_t \cdot EC_t - ue_t \cdot FI_t). \tag{1}$$

Constraints of the problem include the fixed cost condition of the investments (2). Hourly operation of the battery is constrained by the reservoir model (3), the storage capacity (4) and the power limits (5), as well as inequalities precluding simultaneous charging and discharging (6)-(7). PV generation is limited by the installed capacity and the solar irradiation (8). Equation (9) imposes the energy balance of the system.

$$cap_k \leqslant i_k \cdot M$$
 (2)

$$soc_t = soc_{t-1} + ch_t \cdot CEff - \frac{dch_t}{DEff}$$
(3)

$$MiSoc \cdot cap_s \leqslant soc_t \leqslant cap_s$$
 (4)

$$ch_t, dch_t \leqslant cap_s \cdot PCr$$
 (5)

$$ch_t \leqslant \alpha \cdot M$$
 (6)

$$dch_t \leqslant (1 - \alpha) \cdot M \tag{7}$$

$$pv_t \leqslant cap_{pv} \cdot SR_t \tag{8}$$

$$Ld_t = ui_t - ue_t + pv_t + dch_t - ch_t. (9)$$

The above optimization problem is rather simplified, in particular treating demand and DER production as certain, and all costs as known and constant over time. A more realistic setup would be a fully stochastic model for dynamic decision-making that would capture both the intermittent generation and the multiple layers of uncertainty in demand level and DER operations, plus side effects of DER integration saturation and congestion. Our choice is driven by three complementary considerations. First, a fully stochastic model would be orders of magnitude more complicated and would bring a host of computational challenges, taking the focus away from our main topic of the interplay between tariffs and reliability. Second, we emphasize that (2)-(9) optimizes for the behind-the-meter investments to be carried out by consumers. The latter simply do not have the time or the skill to build a sophisticated investment framework, especially relative to a centralized plan that might be adopted by utilities and grid operators. Thus, the DER-CAM model is a streamlined mathematical idealization of the decision making process that might be used (and is actually being used in reality) by prosumers to size their DERs. Third, there is an ongoing overarching debate about the main drivers of behind-the-meter DER adoption with motives ranging from social concerns about clean energy and climate change, to tax and regulatory driven decisions, to concerns about grid security (witness the large-scale forced outages in California during the 2019 fire season). Since capturing all these aspects in the adoption model is beyond the scope of this paper, the DER-CAM formulation presented above should be viewed as a representative example of economics-driven DER adoption serving the purpose of this paper, rather than as *the* most realistic framework to predict DER adoption in a particular area.

3. Reliability Analysis

This section presents a methodology to perform the reliability evaluation for different tariff scenarios and subsequent adoption of PV and storage technologies. This work builds upon existing reliability methods and indices at the level of the distribution grid, which are commonly used in the power systems reliability studies [7, 22]. More detail about this underlying reliability framework can be found in [23].

It is important to stress that our reliability evaluation is based on the adequacy concept of reliability, which is a common technique used for the long-term evaluation in distribution grids reliability [23]. This means that the short-term power quality and security aspects, such as feeders' capacity, as well as voltages in the nodes, are considered to be within limits both with and without adoption of DERs.

3.1. Adoption Model Simulation

We consider a radial distribution network with B buses, denoted $\{b_1, b_2, b_3, \dots, b_B\}$. Each bus contains a consumer with private investments in DERs. Given a tariff, an optimization is run for each consumer, using the model presented in Section 2 to find the optimal portfolio of PV and Storage investments and their dispatch policies. The above determines the decentralized adoption of behind-the-meter DERs; we treat grid-side DERs as fixed, i.e. exogenous to the given distribution network and not affected by the consumer-facing tariffs.

For each bus $b \in \{b_2, b_3, \dots, b_B\}$, the optimization problem is solved locally, independent of the other consumers in the distribution network, considering the data (such as load profile $(Ld_t^b)_{t \in \mathcal{T}_{yr}}$ and tariff $\mathbf{c}_t^b := (EC_t^b, FI_t^b)_{t \in \mathcal{T}_{yr}}$) only for the consumer at bus b. As before, the output of the optimization includes the optimal investments (cap_k^b) , optimal dispatch policy for the storage $(ch_t^b, dch_t^b)_{t \in \mathcal{T}_{yr}}$, PV generation $(pv_t^b)_{t \in \mathcal{T}_{yr}}$, and purchase (export) of power from (to) the utility $(ui_t^b, ue_t^b)_{t \in \mathcal{T}_{yr}}$. As done in [17], by running this optimization we are assuming that each consumer will dispatch storage technologies in a way that minimizes her own costs.

3.2. Monte Carlo Simulation

In this paper, we only consider power interruptions due to failure in the distribution lines and assume the rest of the system components, e.g. storage and PV, to work without any failures, in particular ignoring intermittency in PV generation and any potential overvoltages caused by high solar penetration. Extending our approach to incorporate respective failures would be mathematically straightforward, although computationally intensive. At any time t, we assume that each of the distribution lines $l \in \{1, 2, ..., L\}$ could be in one of the two states, described through the variable δ_t^l , connected ($\delta_t^l = 1$) and disconnected (or failed,

 $\delta_t^l = 0$). We further assume that each distribution line transitions from one state to the other independently, following an Exponential distribution $f_{\tau}(\cdot)$ for the transition times τ_t^l :

$$f_{\tau_t^t}(s) = \tilde{\lambda}_t^l e^{-\tilde{\lambda}_t^l s} \tag{10}$$

where $\tilde{\lambda}_t^l = \lambda_f^l \delta_t^l + \lambda_r^l (1 - \delta_t^l)$. The parameter $\lambda_f^l \in \mathbb{R}_+$ represents the line failure rate, i.e. rate of transition from state $\delta_t^l = 1$ to $\delta_{t+\tau_t^l}^l = 0$, and $\lambda_r^l \in \mathbb{R}_+$ represents the repair rate, i.e. rate of transitions from $\delta_t^l = 0$ to $\delta_{t+\tau_t^l}^l = 1$.

Remark: the network topology is taken to be fixed; the possibility of network reconfiguration or the use of utility owned DERs to minimize impact of line failures has been extensively explored in the literature (e.g. [7] and [22]) and are not considered in our reliability analysis.

The state of the distribution network is defined via $L_t = [\delta_t^1, \delta_t^2, \dots, \delta_t^L]$, which is a vector of states for each distribution line. The time for the next transition of the whole distribution network from state L_t is defined via $\tau_t := \min_l \tau_t^l$ with probability density function

$$f_{\tau_t}(s) = \tilde{\lambda}_t e^{-\tilde{\lambda}_t s},\tag{11}$$

where $\tilde{\lambda}_t = \sum_{l=1}^L \tilde{\lambda}_t^l$ is additive thanks to properties of Exponential random variables. At the transition epoch $t + \tau_t$ the distribution network may transition to L possible states. The probability that the distribution network changes state due to a change in the k^{th} distribution line is:

$$P(\tau_t = \tau_t^k | L_t) = \frac{\tilde{\lambda}_t^k}{\sum_{l=1}^L \tilde{\lambda}_t^l}.$$
 (12)

To assess the reliability of the distribution network, we simulate Monte Carlo samples of the transition times and transition states using Equations (11) and (12). For a total of N_s Monte Carlo samples, we denote by $L_{0:T}^n$, $n = 1, ..., N_s$ the n^{th} sample of the sequence of transition states in the time interval [0, T] and by \mathcal{T}_{fr}^n , $n = 1, ..., N_s$ the corresponding sequence of transition epochs.

Notice that the output of the optimization in Section 2 is defined on the set \mathcal{T}_{yr} containing only hourly time steps, however, the transition times $\mathcal{T}_{fr}^n \in [0,T]$ in any Monte Carlo sample are continuous. As a result, computation of the reliability indices requires analyzing the system for $t \in \mathcal{T}^n := \mathcal{T}_{yr} \cup \mathcal{T}_{fr}^n$. Thus, we extend the output of the optimization problem from $t \in \mathcal{T}_{yr}$ to $t \in [0,T]$ using piecewise constant functions for all the variables, except battery state-of-charge soc_t which is linearly interpolated:

$$soc_{t} = soc_{t_{j}-1} + ch_{t_{j}} \cdot CEff - \frac{dch_{t_{j}}}{DEff} \cdot (t_{j} - t) \quad \forall t \in [t_{j}, t_{j+1}) \quad \text{and } t_{j} \in \mathcal{T}_{yr}.$$

$$(13)$$

3.3. Network Representation During Failures

A distribution network can be represented as a graph with vertices $\{v_1, \ldots, v_B\}$ representing the buses $\{b_1, \ldots, b_B\}$, and the edges $\{e_1, e_2, \ldots, e_L\}$ representing the distribution lines $\{l_1, l_2, \ldots, l_L\}$. This transformation is useful when considering large networks with thousands of buses and distribution lines. Since we only consider radial networks in this paper, the corresponding graph is an acyclic tree. A failure at any

distribution line is equivalent to "breaking" the edge in the corresponding tree, partitioning it into two compartments. At any time t, we represent the total number of compartments as $A_t \ge 1$ and $\mathcal{I}_{i,t}$, $i = 1, \ldots, A_t$ representing the set of vertices in compartment i.

The overall set of compartments at time t is denoted by $\mathcal{A}_t = \{\mathcal{I}_{1,t}, \dots, \mathcal{I}_{A_t,t}\}$, where $\mathcal{I}_{1,t}$ is the set of all vertices which have a path to v_1 (substation); it corresponds to buses with uninterrupted supply of power from the utility even after line failure(s). The buses corresponding to vertices $v \notin \mathcal{I}_{1,t}$ have no connection to the utility at t. For this set of buses, consumers with no DERs, or only PV installed, experience a power outage. In contrast, consumers with storage devices installed behind the meter are able to supply their loads in isolation. Assumptions on the respective islanded operation are presented next.

3.4. Storage dispatch policy during outages

Line outages will force behind-the-meter storage devices to work in an islanded mode, prioritizing the supply of consumers' load. Therefore, due to multi-period nature of the optimal dispatch given by $(\operatorname{ch}_t^b, \operatorname{dch}_t^b)_{t\geqslant 0}$ (again, superscript b to emphasize that it is specific to the storage at bus b), an outage affects the dispatch policies in subsequent times.

To address this issue, an optimal re-dispatch policy should be run for each islanded storage device and for each outage. However, given the number of outages and nodes in the system, this would increase exponentially the computational complexity of the simulation. Instead, we propose a heuristic in order to keep the operational conditions of the storage device as close as possible to the original optimal dispatch calculated with the adoption model presented in Section 2.

We denote the operational policy for the charge and discharge of the storage at bus b via $(\widehat{ch}_{t_j}^b)_{t_j \in \mathcal{T}}$ and $(\widehat{dch}_{t_j}^b)_{t_j \in \mathcal{T}}$ respectively (using \hat{c} to remind that it is different from the optimal); and the corresponding state of charge as $(\widehat{soc}_{t_j}^b)_{t_j \in \mathcal{T}}$. Let us define an additional state variable $(m_{t_j}^b)_{t_j \in \mathcal{T}}$, which determines the operational policy $(\widehat{ch}_{t_j}^b, \widehat{dch}_{t_j}^b)_{t_j \in \mathcal{T}}$ of the storage:

$$m_{t_j}^b = \begin{cases} 1 & \text{if } b \in \mathcal{I}_{1,t_j} \text{ and } \widehat{soc}_{t_j}^b = soc_{t_j}^b \\ 2 & \text{if } b \notin \mathcal{I}_{1,t_j} \\ 3 & \text{if } b \in \mathcal{I}_{1,t_j} \text{ and } \widehat{soc}_{t_j}^b \neq soc_{t_j}^b. \end{cases}$$

$$(14)$$

The three cases in (14) determine the three modes: normal, active, and recovery.

- Normal $(m_{t_j}^b = 1)$: During this mode, the bus is connected to the utility $b \in \mathcal{I}_{1,t_j}$, and state of charge is same as the optimal $\widehat{soc}_{t_j} = soc_{t_j}$. As a result, the dispatch follows the optimal control policy as derived from the optimization in Section 2, i.e. $\widehat{ch}_{t_j}^b = ch_{t_j}^b$, $\widehat{dch}_{t_j}^b = dch_{t_j}^b$.
- Active $(m_{t_j} = 2)$: storage transitions to a back-up mode when the bus b has no connection to the utility $b \notin \mathcal{I}_{1,t_j}$. During back-up the storage unit acts to balance the net demand (load PV generation), supplying power when net demand > 0 and charging when net demand < 0 while being constrained

by the physical limits of the storage unit. We assume that the storage control at time t_j is determined by the information available only prior to t_j , i.e. at the time of failure, so the policy does not depend on the time-to-repair and assumes the failure will continue at least until the nearest hourly time-step. Thus, the storage policy is given by:

$$\widehat{dch}_{t_j}^b = \left((Ld_{t_j}^b - pv_{t_j}^b) \wedge \widehat{dch}_{t_j}^{b, \max} \right)^+; \tag{15}$$

$$\widehat{ch}_{t_j}^b = \left((pv_{t_j}^b - Ld_{t_j}^b) \wedge \widehat{ch}_{t_j}^{b, \max} \right)^+, \tag{16}$$

where

$$\widehat{dch}_{t_j}^{b,\max} = \left[cap^b \cdot PCr \right] \wedge \left[\left(soc_{t_j}^b - MiSoc \cdot cap^b \right) \frac{DEff}{\left[t_j \right] - t_j} \right]; \tag{17}$$

$$\widehat{ch}_{t_j}^{b,\max} = \left[cap^b \cdot PCr \right] \wedge \left[\frac{cap^b - soc_{t_j}^b}{CEff \cdot ([t_j] - t_j)} \right]$$
(18)

and $x \wedge y$ and $(x)^+$ are shorthand notations for $\min(x,y)$ and $\max(x,0)$ respectively.

• Recovery $(m_{t_j}^b = 3)$: bus b is connected to the utility $b \in \mathcal{I}_{1,t}$, but its operational state of battery charge is different from the optimal, $\widehat{soc}_{t_j}^b \neq soc_{t_j}^b$. Within this mode the charge/discharge policy aims to get the operational soc back to the optimal. Namely, if the operational soc is higher than the optimal, $soc_{t_j}^b - \widehat{soc}_{t_j}^b > 0$, the customer sells energy to the grid when re-connection occurs.

$$\widehat{ch}_{t_j}^b = \left(\frac{soc_{\lfloor t_j \rfloor}^b - \widehat{soc}_{t_j}^b}{CEff \cdot (\lceil t_j \rceil - t_j)} \wedge \widehat{ch}_{t_j}^{b, \max}\right)^+. \tag{19}$$

Conversely, when $soc^b_{\lceil t_j \rceil} - \widehat{soc}^b_{t_j} < 0$:

$$\widehat{dch}_{t_j}^b = \left(\frac{(\widehat{soc}_{t_j}^b - soc_{\lfloor t_j \rfloor}^b) \cdot DEff}{(\lfloor t_j \rfloor - t_j)} \wedge \widehat{dch}_{t_j}^{b, \max}\right)^+. \tag{20}$$

Finally, given the operational policy of the storage, the \widehat{soc} updates via:

$$\widehat{soc}_{t_{j+1}} = \widehat{soc}_{t_j} + \left(\widehat{ch}_{t_j} \cdot CEff - \frac{\widehat{dch}_{t_j}}{DEff}\right) \cdot (t_{j+1} - t_j). \tag{21}$$

3.5. Reliability indices

In this section we discuss the computation of reliability indices. We only consider active power, with no losses, and assume that during outages the voltage at each bus connected to the utility grid is within the security limits. These assumptions are common in reliability studies of distribution networks [14, 17].

Given a Monte Carlo sample of the transition times \mathcal{T}^n and states $L_{0:T}^n$, the first step is to evaluate the loss of load $C_{t_j}^{b,n}$ for the bus b at time $t \in [0,T]$. We define $C_t^{b,n}$ as:

$$C_{t}^{b,n} := \begin{cases} 0 & \text{if } b \in \mathcal{I}_{1,t}^{n}; \\ Ld_{t}^{b} & b \notin \mathcal{I}_{1,t}^{n}, cap_{s}^{b} = 0; \\ (Ld_{t}^{b} - pv_{t}^{b} - \widehat{dch}_{t}^{b,n} + \widehat{ch}_{t}^{b,n})^{+} & b \notin \mathcal{I}_{1,t}^{n}, cap_{s}^{b} > 0. \end{cases}$$

$$(22)$$

According to (22), the consumer at bus b does not experience interruptions, $C_t^{b,n}=0$, if connected to the utility $b\in\mathcal{I}_{1,t}^n$. However, if a line failure occurs between the bus and the substation, $b\notin\mathcal{I}_{1,t}^n$, and there is no local storage, $cap_s^b=0$, the outage experienced by the consumer is equal to the load demand Ld_t^b . The implicit assumption is that the PV, due to voltage and frequency stability reasons, requires either the grid or additional storage to feed the load. If neither is available, the circuit breaker connecting the PV to the consumer trips and the loss of load experienced by the consumer is equal to the demand. Finally, if the node is not connected but a storage unit is installed locally, $cap_s>0$, the loss of load will be equal to the net demand after storage re-dispatch.

The traditional indices used to assess the reliability of the distribution systems, such as the average energy not supplied (AENS) and the system average interruption duration index (SAIDI), are focused on the evaluation of the performance of the utility network. Thus, if a failure occurs, the immediate loss of load that results from the event is assigned to these indices. However, with the presence of behind-the-meter DERs, especially PV and storage technologies, at least part of this load can be recovered during a grid failure event, mitigating the loss of load that is actually experienced by the consumer. This creates an apparent paradox: on the one hand, the consumer experiences less load curtailment; on the other hand, the distribution network does not become more "reliable", as its failure pattern and its performance do not change. Therefore, to better translate this reality, it is necessary to create additional indices that capture the performance of the joint system, composed by the distribution grid and the behind-the-meter DERs, and express the actual failures experienced by the consumers. In this paper, we create two indices with these characteristics and name them average energy not consumed (AENC) and average outage duration index (AODI). Similar to the standard AENS, AENC computes the average energy interruptions that are actually experienced by the consumer. Analogously, AODI corresponds to the SAIDI, but accounting for the duration of the outages actually experienced by the consumer. Thus, when considering behind-the-meter DER adoption driven by rate design, AODI will be impacted by the incentives for storage installation provided by the tariff, while SAIDI remains the same regardless of the rate design decisions, as it only depends on the characteristics of the distribution grid failures.

Thus, we employ the standard definitions of energy not supplied $\text{ENS}^{b,n}(\mathbf{c}^b)$ and duration of the interruptions from the perspective of the utility $\text{ID}^{b,n}(\mathbf{c}^b)$, plus introduce energy not consumed $\text{ENC}^{b,n}(\mathbf{c}^b)$ and the consumer outage duration $\text{OD}^{b,n}(\mathbf{c}^b)$ at the bus b for the n^{th} Monte Carlo sample as:

$$ENS^{b,n}(\mathbf{c}^b) := \int_0^T u i_t^b \mathbf{1}_{b \notin \mathcal{I}_{1,t}^n} dt, \tag{23}$$

$$\mathrm{ID}^{b,n}(\mathbf{c}^b) := \int_0^T \mathbf{1}_{\{b \notin \mathcal{I}_{1,t}^n\}} \mathrm{dt},\tag{24}$$

$$ENC^{b,n}(\mathbf{c}^b) := \int_0^T C_t^{b,n} dt, \tag{25}$$

$$\mathrm{OD}^{b,n}(\mathbf{c}^b) := \int_0^T \mathbf{1}_{\{C_t^{b,n} > 0\}} \mathrm{dt}. \tag{26}$$

 $\mathrm{ENS}^{b,n}$ accounts for the total energy that the utility could not supply to bus b during the period [0,T].

 $\mathrm{ENC}^{b,n}$ and $\mathrm{OD}^{b,n}$ quantify, respectively, the loss of load and the outage duration for the consumer after incorporating the re-dispatch from the storage. Equations (23)-(26) emphasize the dependence of these metrics on the tariffs \mathbf{c}^b .

To clarify the definition of $ENS^{b,n}(\mathbf{c}^b)$ and $ENC^{b,n}(\mathbf{c}^b)$, Table 1 summarizes the relationship between these indices for different investment scenarios at bus b. As shown in the table, when only PV is installed behind the meter, the ENC is higher than the ENS. This occurs since the demand at b seen by the utility right before a failure is the net load, while the actual outage experienced by the consumer corresponds to the total load due to the disconnection of PV.

Investment Relationship between ENS and ENC

None $ENS^{b,n}(\mathbf{c}^b) = ENC^{b,n}(\mathbf{c}^b)$ Only PV $ENS^{b,n}(\mathbf{c}^b) \leqslant ENC^{b,n}(\mathbf{c}^b)$ PV and storage $ENS^{b,n}(\mathbf{c}^b) \geqslant ENC^{b,n}(\mathbf{c}^b)$

Table 1: Relationship between ENS and ENC

Finally, a generic reliability index with B buses in the distribution network can be defined as:

Index :=
$$\frac{1}{N_s} \sum_{n=1}^{N_s} \left[\frac{\sum_{i=2}^{B} F^{b_i, n}}{B} \right],$$
 (27)

$$\sigma(\text{Index}) = \frac{\sqrt{\sum_{n=1}^{N_s} \left[\frac{\sum_{i=2}^{B} F^{b_i, n}}{B} - \text{Index}\right]^2}}{N_s},$$
(28)

where $F^{b_i,n}$ is a test function. Thus, Index computes the average of the test function over the buses and the N_s Monte Carlo samples and $\sigma(\text{Index})$ is the standard error in estimating the index. If the test function is $\text{ENS}^{b_i,n}(\mathbf{c}^{b_i})$, then the corresponding index is AENS; if it is $\text{ID}^{b_i,n}(\mathbf{c}^{b_i})$, then the index is SAIDI; if it is $\text{ENC}^{b_i,n}(\mathbf{c}^{b_i})$, then the index is AENC; and if it is $\text{OD}^{b_i,n}(\mathbf{c}^{b_i})$, then the index is AODI.

3.6. Algorithm

We summarize the overall sequence of steps to compute the reliability indices in Algorithm 1. Line 2 calls the adoption model of Section 2 for computing the optimal investment in DERs and their dispatch policy. Lines 4-10 compute the ENS, FD, ENC and OD for every bus in the network given a Monte Carlo sample of sequence of failure repair times for the distribution lines. Lines 6-8 compute the loss of load at each transition time (or hourly time step) in the Monte Carlo sample. Line 12 computes the reliability indices by averaging over all the buses and samples.

Algorithm 1 Monte Carlo simulation for reliability computation

```
1: Input: Distribution network, load demand for consumers
                tariff rates, failure and repair rates.
 2: Solve the optimization problem from Sec. 2 for each bus b = 2, 3, \dots, B.
 3: for n = 1, 2, ..., N_s do
       Simulate set of failure-repair times \mathcal{T}_{fr}^n on [0,T] (Sec. 3.2).
 4:
       for t \in \mathcal{T}^n := \mathcal{T}_{yr} \bigcup \mathcal{T}_{fr}^n do
 5:
          Find the set of buses \mathcal{I}_{1,t} connected to substation (Sec. 3.3).
 6:
          Compute storage dispatch \widehat{dch}_t^{b,n}, \widehat{ch}_t^{b,n}, b = 2, 3, \dots, B (Sec. 3.4).
 7:
          Calculate C_t^{b,n} for b=2,3,\ldots,B using Eqn (22).
 8:
       end for
 9:
       Compute ENS^{b,n}, FD^{b,n}, ENC^{b,n} and OD^{b,n} (Eqns (23)-(26)).
11: end for
12: Calculate indices: AENS, SAIDI, AENC and AOD via Eqn (27).
13: return: AENS, SAIDI, AENC, AOD
```

4. Results

4.1. Case Study

This section discusses the effect of different tariff structures on the adoption of PV and storage technologies by private consumers, along with the consequent impact on the reliability of the system, both from the perspective of the consumers and the utility. We consider the modified PG&E 69-bus [24][25] MV network (Figure 1), where each node connects either a Commercial complex (blue diamonds), a public service building (green circles) or a block of Midrise Apartment buildings (red triangles). Annual load profiles were obtained from the 16 DOE Reference buildings database for the climate zone of San Francisco [26]. From the database, hospital, offices and school profiles were considered public service, while the remaining (with the exception of the Midrise Apartment) were assumed commercial. Load profiles were scaled to fit original network load [24] at 8:00am on the first day of January. The total annual energy consumption is ≈ 23 GWh.

PV radiation data was obtained from Typical Meteorological Year 3 datasets for the same geographical area [27]. We assume the fixed cost $CFix_{pv}$ and variable $CVar_{pv}$ cost as \$2500 and 2500\$/kWh respectively and a PV lifetime of 20 years. We consider a storage charging/discharging efficiency (CEff/DEff) of 0.9, a maximum charge/discharge rate PCr of 0.3 kW per kWh installed, and minimum state of charge MiSoc of 0.2. Due to the relatively small rate of charge/discharge, relatively low costs of storage are assumed: fixed cost $CFix_s = 250 and variable cost $CVar_s = 250$ \$/kWh respectively. Lifetime of the batteries is considered to be 10 years and to simplify the analysis the effect of energy degradation due to calendar and cycle capacity losses is neglected. However, adding this effect is straightforward, for example using the methodological framework proposed in [28].

The base purchase rate EC_t for the different consumer classes (residential, services and commercial) is

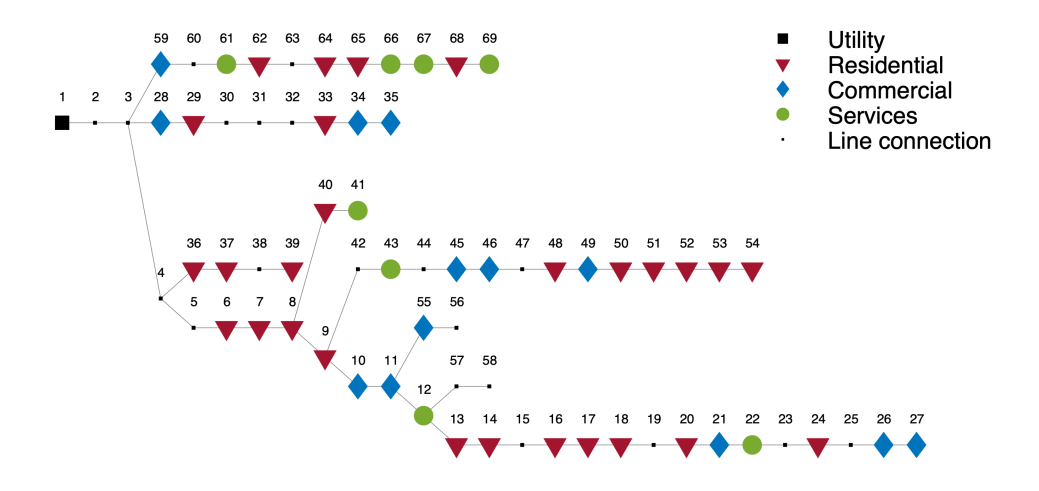


Figure 1: Modified PG&E 69-bus system [25] with 3 customer types.

presented in Table 2. Residential tariffs have only two blocks of Time-of-use rates (on-peak and off-peak), while service and commercial consumers have a three-segment tariff structure, divided into on-peak, mid-peak and off-peak hours. The peak purchase rate for the residential consumers is during the evening from 4:00pm - 9:00pm, while service and commercial consumers have peak purchase rate during the day from noon-6:00pm. For all classes of consumers the feed-in remuneration, FI_t , received at time t for exporting energy to the utility grid is considered to be 30% of the energy cost shown in Table 2.

We use $N_s = 500$ Monte Carlo samples on the time horizon of 1 year, [0, 8760] hours, to compute all the reliability metrics.

4.2. Base Case Results

Table 3 presents the four system reliability indices, considering the base case tariffs for each type of consumer. For comparison purposes, three scenarios of investment were assumed: (A) no investments by the consumer are allowed and only the original load is considered for the calculation of the indices; (B) the consumers are allowed to make optimal investments, but only in PV; (C) optimal adoption of both PV and Storage.

As presented in the Table, AENS significantly decreases when PV investments are allowed, since the energy dependence on the utility is reduced. When storage is added to the system in scenario (C), AENS keeps decreasing. This is explained by the incentive for self-consumption that is implicit in the tariff, with a feed-in remuneration 30% lower than the energy costs. Thus, the presence of storage avoids some PV injection during the daylight hours, allowing the use of this energy in subsequent periods and decreasing the total energy required from the utility grid. By observing the distribution of AENS for the 3 scenarios (left panel of Figure 2), it is possible to conclude that the PV investments, both alone or combined with storage, also reduce the variance of the index.

Table 2: Base tariff rates and periods for different classes of consumers

Type	Weekdays	Weekends	Summer	Winter
			(\$/kWh)	(\$/kWh)
	Residential Tariff		Jun-Sep	Oct-May
On-peak	4:00pm - 9:00pm	_	0.36335	0.22588
Off-peak	Other times	All times	0.26029	0.20708
	Services Tariff		May-Oct	Nov-April
On-peak	noon - 6:00pm	_	0.14726	0.10165
Mid-peak	8:00am - noon 6:00pm - 9:00pm	_	0.10714	0.10165
Off-peak	9:00 pm - 8:00 am	All times	0.08057	0.08717
Commercial Tariff			May-Oct	Nov-April
On-peak	noon - 6:00 pm	_	0.21471	0.1309
Mid-peak	8:00am - noon 6:00pm - 9:00pm	_	0.15958	0.1309
Off-peak	9:00pm - 8:00am	All times	0.13151	0.11384

Table 3: Reliability Indices and Investment Scenarios (base case)

Scenario	AENS	SAIDI	AENC	AODI	PV	Storage
	(kWh)	(hours)	(kWh)	(hours)	(kW)	(kWh)
No DERs	526.3	12.1	526.3	12.1	0	0
PV only	378.8	12.1	526.3	12.1	3,812	0
PV+Storage	355.8	12.1	417.4	9.5	3,812	3,852

In contrast, as shown in Table 3, the magnitude and the duration of the outages experienced by the consumers (AENC and AODI) only decrease when storage is added to the system. This reduction also occurs in terms of the variance of the indices, illustrated in Figure 2 (right panel). Without storage, PV is not able to operate in islanded mode during a line failure in the distribution grid, which results in the entire loss of load for the consumers. From the utility perspective, the magnitude of the interruption considered during a failure is the net load, which justifies the difference between AENS and AENC observed in Table 3.

In scenario (C), the adoption of storage by some consumers partially rectifies this difference, decreasing the AENC and the AODI. However, the AENC is still significantly higher than the AENS, which means that the base case tariff is not able to incentivize storage investments in all consumer segments. Indeed, the computation of the hourly indices in Figure 3 shows a considerable difference between AENC and AENS

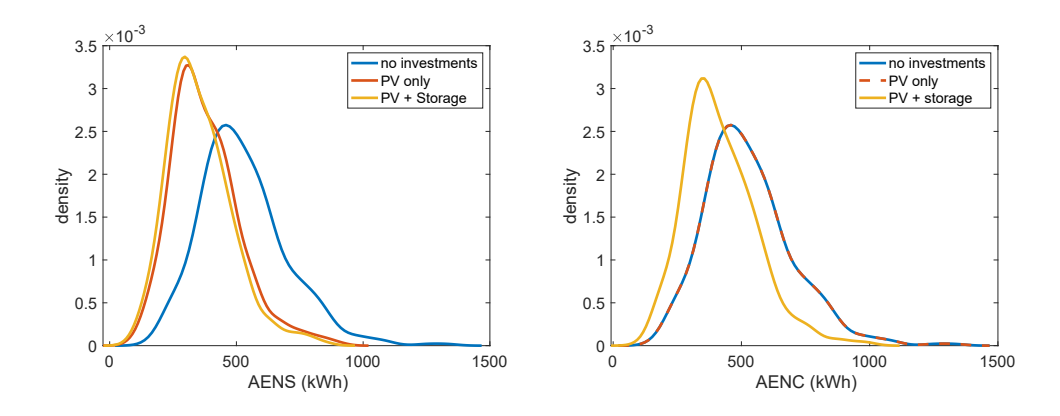


Figure 2: Distribution of AENS for the 3 scenarios (left); Distribution of AENC for the 3 scenarios (right).

during the daylight periods, indicating that most of the consumers invest only in PV technologies.

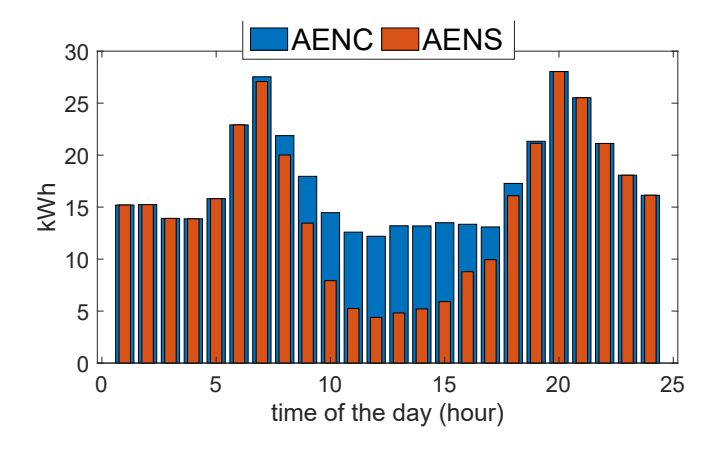


Figure 3: Hourly indices for scenario (C).

To better understand the impact of the tariff incentives on the reliability of the system via adoption of PV and storage, a sensitivity analysis to different tariff components is conducted in the following subsections. For ease of presentation, we restrict ourselves to univariate analysis, modifying one tariff component at a time. More comprehensive multivariate sensitivities are left to future research. Because running our model is computationally intensive, we advocate the application of statistical surrogates to investigate multiple sensitivities simultaneously so as to identify optimal tariffs.

4.3. Homothetic variation of energy tariffs

The variation of the energy tariff offered by the utility affects the economic conditions for adoption of DERs by private consumers. As shown in the previous section, this adoption has an impact on the system reliability indices, both from the perspective of the utility and of the consumers.

By defining the energy cost rates presented in the base case tariff as $\overline{\mathrm{EC}}_t$, the homothetic variation can be described by $\mathrm{EC}_t = \gamma_{\mathrm{pur}} \cdot \overline{\mathrm{EC}}_t \quad \forall t \in [0,T]$, where γ_{pur} represents the variation factor of the energy

purchase costs for consumers. In this analysis, we allow a variation of 30% of this purchase cost factor, i.e. $0.7 \le \gamma_{\text{pur}} \le 1.3$.

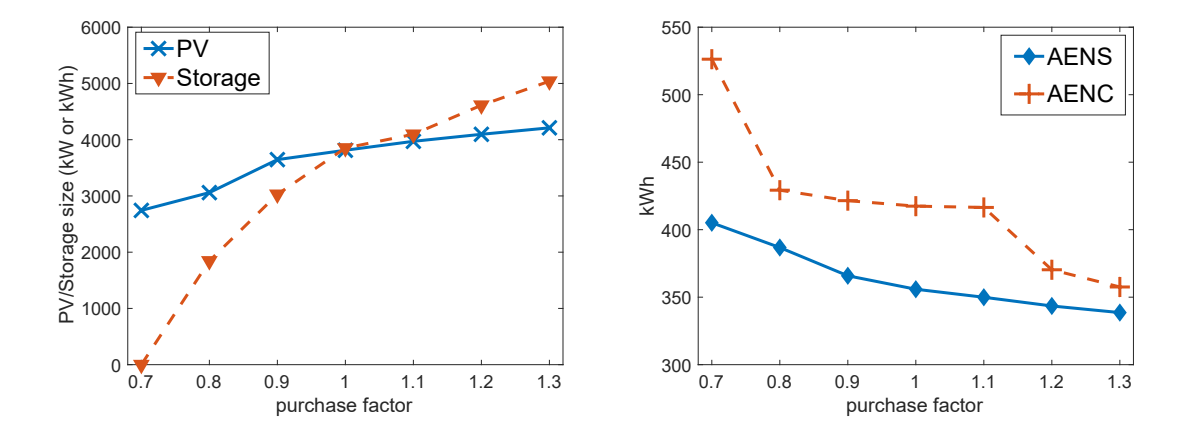


Figure 4: Effect of γ_{pur} on DER investments cap_{pv} and cap_s (left) and reliability (right).

Figure 4 presents the adoption of PV and storage as a function of the homothetic variation of the energy costs, as well as the consequent impact on AENS and AENC. Although both PV and storage capacity increase with the energy rates, PV is already cost-effective at 70% of costs, while storage requires higher rates to become economically worthwhile. As expected, AENS decreases as consumption depends less on the utility and more on the on-site PV generation, whereas the magnitude of outages experienced by the consumers (AENC) only decreases with the adoption of storage. However, it is possible to observe that this effect does not have a linear characteristic, i.e. initial adoption of storage has little impact on AENC, which indicates that the reliability benefits for consumers from storage adoption depend not only on the available capacity, but also on its utilization throughout the day. Therefore, the next subsection will analyze the reliability impact of the time component variation of tariffs.

4.4. Time differentiation of energy rates

In this section we consider a variation in the ToU component of the tariff by increasing the cost of energy during the peak hours and keeping constant the off-peak and mid-peak rates. Similar to the previous analysis, we use a peak ratio, γ_{pk} , to describe this variation and represent the energy costs as:

$$EC_{t} = \begin{cases} \gamma_{pk} \cdot \overline{ECt}_{t} & \text{if } t \in \mathcal{T}_{pk}; \\ \overline{ECt}_{t} & \text{if } t \notin \mathcal{T}_{pk}, \end{cases}$$

$$(29)$$

where \mathcal{T}_{pk} is the set of times corresponding to on-peak periods presented in Table 2. Since the on-peak component of the ToU only lasts 5 hours for residential and 6 hours for commercial and services consumers, we allowed a variation up to 250% of these costs: $1.0 \leq \gamma_{pk} \leq 2.5$.

Figure 5 shows the effect of this variation on the DER investments (cap_{pv}, cap_s) and the consequent impact on reliability indices. Increasing γ_{pk} raises aggregate investments in storage up to 400% (3,852 kWh

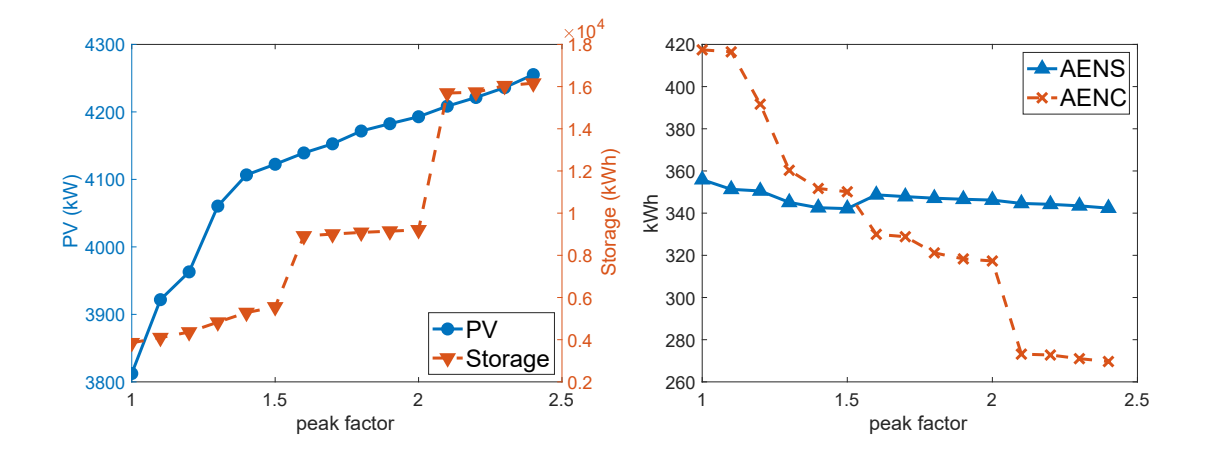


Figure 5: Effect of γ_{pk} on DER investments (left panel: cap_{pv} and cap_s on the left and right y-axis respectively) and reliability (right panel).

to 16,162 kWh), but has only moderate impact on the adoption of PV (from 3,812 kW to 4,255 kW). Thus, a significant differentiation between off/mid peak and on-peak rate creates a stronger incentive for storage adoption than for additional PV capacity. We note jumps in the capacity of the storage investments as a function of $\gamma_{\rm pk}$ as ToU differentiation becomes relevant for more and more classes of consumers. From a reliability perspective, AENS remains practically constant, meaning that the overall dependence on the utility changes minimally, due to the insignificant variation in PV investments. In contrast, AENC decreases significantly as storage capacity is introduced. However, Figure 6 shows that the average outages experienced by the consumers do not decrease uniformly throughout the day. When comparing the base tariff against a scenario where peak costs are doubled, it is possible to observe a reduction on AENC during the day/evening hours and no improvements during the night.

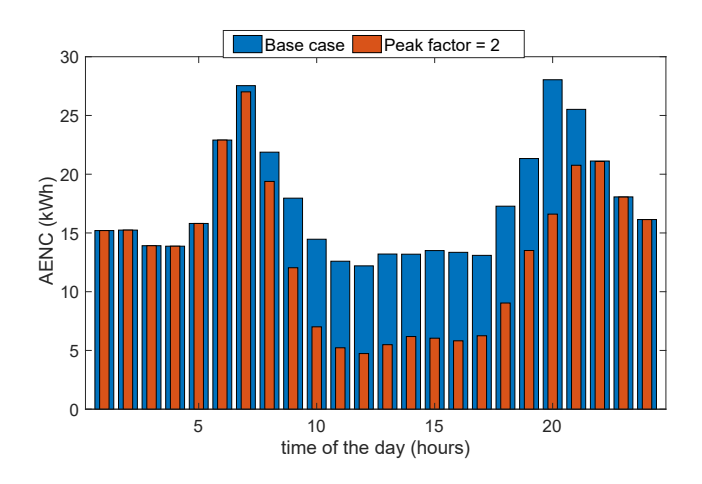


Figure 6: Impact of ToU differentiation on hourly distribution of AENC: base case vs. peak factor $\gamma_{\rm pk}=2$.

This can be explained by the storage dispatch policy generated from an extremely differentiated ToU

structure that incentivizes consumers to buy energy during the morning and keep the batteries full until the on-peak period. Therefore, if a failure occurs during the day, behind-the-meter batteries will be full and able to drastically minimize the impact of the outage on the consumers. This situation persists until the end of peak period when batteries fully discharge and storage no longer can buffer line failures.

Thus, thanks to their capability to influence storage adoption, rate design policies comprising time differentiation of costs are an effective solution to improve AENC. This can be seen in Figure 7 which compares homothetic variation of Section 4.3 with the energy costs differentiation scenarios analyzed above with respect to their impact on AENC and on the overall annual costs of the consumers. We find that for the same annualized costs—see equation (1)—the AENC is considerably lower when differentiation is included in rate design.

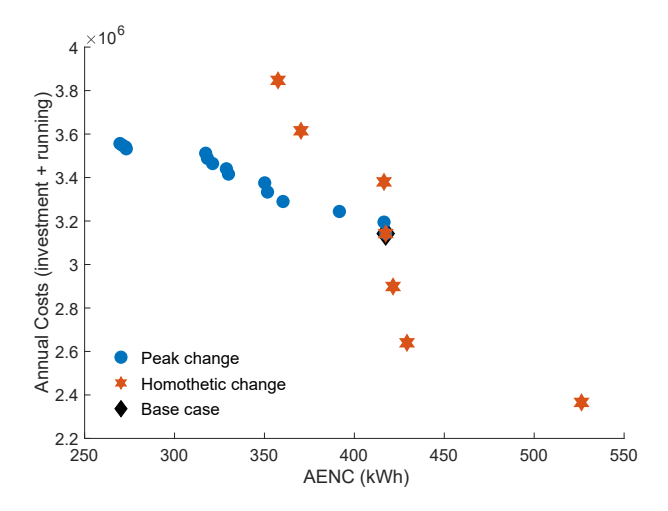


Figure 7: Impact of homothetic variation and cost differentiation policies on consumers' annual costs and consequent effect on AENC. Blue dots correspond to different values of $\gamma_{\rm pk} \in [1,2]$, orange stars to different values of $\gamma_{\rm pur} \in [0.7,1.3]$ and the black diamond to the base scenario with $\gamma_{\rm pk} = \gamma_{\rm pur} = 1$.

4.5. Shifting time-of-use periods

Our last analysis consists of shifting in time the on-peak component of the ToU rate applied to the residential consumers, keeping the peak costs and duration (5 hours) equal to the base case. Thus, instead of starting at 4PM, four additional possibilities to start the residential on-peak period are explored: 8AM, 10AM, 12PM and 2PM. Figure 8 shows that this shift has little effect on the PV penetration cap_{pv} , but a significant impact on storage adoption cap_s , namely storage investments decrease dramatically when the on-peak period is moved to the morning. Indeed, in this situation, the on-peak energy costs overlap with the solar generation period, reducing the net load when energy costs are higher and dispensing the need for larger storage capacities.

In particular, when the on-peak starts at 8AM, it still ends within the daylight period (1PM), allowing batteries to re-charge using PV generation, and subsequently keeping a full soc until the peak of the next

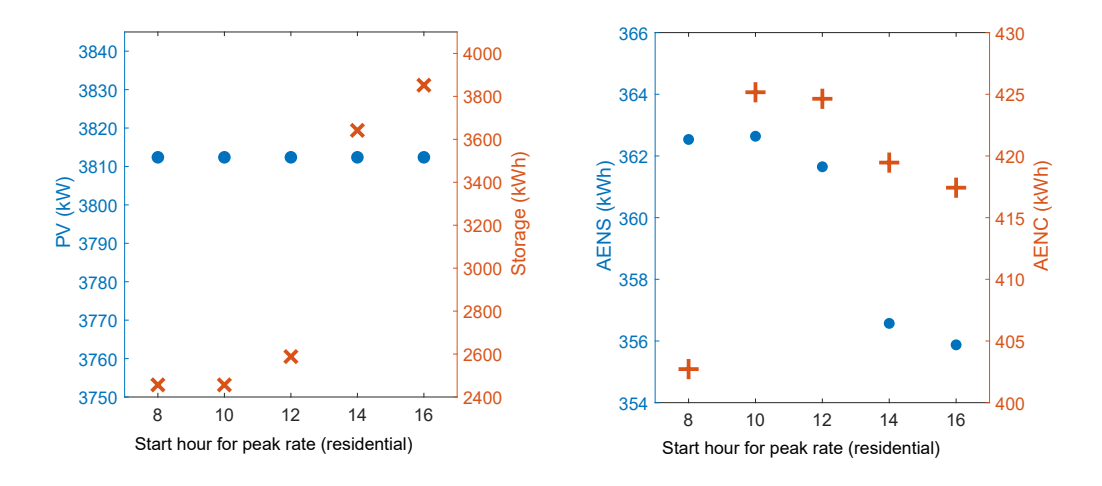


Figure 8: Effect of shifting the on-peak period of residential tariffs on DER investments (left) and reliability (right).

morning. This long period at full capacity mitigates the impact of outages on consumers when a grid failure occurs during the evening/night, resulting in a low value of AENC. When the on-peak period starts at 4PM, there is almost no incentive to charge the batteries before the morning, making consumers more vulnerable to grid failures during the night. However, since the batteries are empty in the morning, the PV self-consumption can be maximized, reducing the overall net load purchased from the utility and decreasing the AENS.

5. Conclusion

This paper presented a methodology to quantify the effect of rate design on the long term reliability of power distribution, assuming that electricity tariffs will become a main driver for adoption of DERs (e.g. PV and storage) by private consumers.

Our results show that both magnitude and structure of time-of-use electricity rates influence the adoption and the dispatch of behind-the-meter DERs with significant impact on the outages accounted by the utility and experienced by the consumers. In general, tariffs incentivizing PV adoption will tend to reduce the overall consumers' dependence on the grid, decreasing the energy-related reliability indices considered by the utility. In contrast, tariffs incentivizing the adoption of storage technologies, such as ToU rates, tend to mitigate the impact of grid failures on the actual loss of load. Here, the magnitude and temporal aspects of cost differentiation play a major role on the hourly distribution of the outages experienced by the consumers. Thus, in many cases, the rate design process can lead to contradictory reliability effects, depending whether the indices are quantified from the perspective of the utility or of the consumer. This phenomenon reinforces the need to rethink current regulatory frameworks in the context of mass adoption of DERs. Additionally, different consumers have distinct sensitivities of reliability to electricity rates. As a result, methodology to quantify the impact of electricity rates on reliability, as in this paper, can provide targeted guidance for

policy making.

Additional analysis is required for alternative pricing mechanisms, such as dynamic pricing and demand response policies that might become more prevalent over time.

Acknowledgment

The authors would like to acknowledge Dan Ton and Ali Ghassemian, Program Managers at the U.S. Department of Energy - Office of Electricity, for the support granted to this work through the Microgrid R&D Program and the Advanced Grid Modeling Program. Aditya Maheshwari and Michael Ludkovski were supported in part by NSF DMS-1736439. We thank the editorial team for several helpful suggestions to improve the manuscript.

References

- [1] IPCC, Special Report on Renewable Energy Sources and Climate Change Mitigation, Cambridge University Press, 2011, Ch. 8, pp. 609–706 (2011).
- [2] California Energy Commission, Building Energy Efficiency Standards for Residential and Nonresidential Buildings (2019).
- [3] R. Sioshansi, Retail electricity tariff and mechanism design to incentivize distributed renewable generation, Energy Policy 95 (2016) 498 508 (2016).
- [4] A. Picciariello, J. Reneses, P. Frias, L. Söder, Distributed generation and distribution pricing: Why do we need new tariff design methodologies?, Electric Power Systems Research 119 (2015) 370 376 (2015). doi:https://doi.org/10.1016/j.epsr.2014.10.021.
- [5] S. Candas, K. Siala, T. Hamacher, Sociodynamic modeling of small-scale PV adoption and insights on future expansion without feed-in tariffs, Energy Policy 125 (2019) 521 536 (2019).
- [6] D. W. Cai, S. Adlakha, S. H. Low, P. D. Martini, K. M. Chandy, Impact of residential PV adoption on retail electricity rates, Energy Policy 62 (2013) 830 – 843 (2013). doi:https://doi.org/10.1016/j. enpol.2013.07.009.
- [7] D. Issicaba, J. A. Pecas Lopes, M. A. da Rosa, Adequacy and security evaluation of distribution systems with distributed generation, IEEE Transactions on Power Systems 27 (3) (2012) 1681–1689 (Aug 2012).
- [8] A. M. Leite da Silva, L. C. Nascimento, M. A. da Rosa, D. Issicaba, J. A. Peças Lopes, Distributed energy resources impact on distribution system reliability under load transfer restrictions, IEEE Transactions on Smart Grid 3 (4) (2012) 2048–2055 (Dec 2012). doi:10.1109/TSG.2012.2190997.

- [9] H. Farzin, M. Moeini-Aghtaie, M. Fotuhi-Firuzabad, Reliability studies of distribution systems integrated with electric vehicles under battery-exchange mode, IEEE Transactions on Power Delivery 31 (6) (2016) 2473–2482 (Dec 2016).
- [10] H. Farzin, M. Fotuhi-Firuzabad, M. Moeini-Aghtaie, Reliability studies of modern distribution systems integrated with renewable generation and parking lots, IEEE Transactions on Sustainable Energy 8 (1) (2017) 431–440 (Jan 2017).
- [11] N. Z. Xu, C. Y. Chung, Reliability evaluation of distribution systems including vehicle-to-home and vehicle-to-grid, IEEE Transactions on Power Systems 31 (1) (2016) 759–768 (Jan 2016). doi:10.1109/ TPWRS.2015.2396524.
- [12] A. Safdarian, M. Z. Degefa, M. Lehtonen, M. Fotuhi-Firuzabad, Distribution network reliability improvements in presence of demand response, IET Generation, Transmission Distribution 8 (12) (2014) 2027–2035 (2014).
- [13] K. I. Sgouras, D. I. Dimitrelos, A. G. Bakirtzis, D. P. Labridis, Quantitative risk management by demand response in distribution networks, IEEE Transactions on Power Systems 33 (2) (2018) 1496–1506 (March 2018).
- [14] H. Farzin, M. Fotuhi-Firuzabad, M. Moeini-Aghtaie, Role of outage management strategy in reliability performance of multi-microgrid distribution systems, IEEE Transactions on Power Systems 33 (3) (2018) 2359–2369 (May 2018).
- [15] R. Li, Q. Wu, S. S. Oren, Distribution locational marginal pricing for optimal electric vehicle charging management, IEEE Transactions on Power Systems 29 (1) (2014) 203–211 (Jan 2014). doi:10.1109/ TPWRS.2013.2278952.
- [16] S. Huang, Q. Wu, M. Shahidehpour, Z. liu, Dynamic power tariff for congestion management in distribution networks, IEEE Transactions on Smart Grid 10 (2) (2019) 2148–2157 (March 2019).
- [17] M. Rastegar, Impacts of residential energy management on reliability of distribution systems considering a customer satisfaction model, IEEE Transactions on Power Systems 33 (6) (2018) 6062–6073 (Nov 2018). doi:10.1109/TPWRS.2018.2825356.
- [18] M. Chesser, J. Hanly, D. Cassells, N. Apergis, The positive feedback cycle in the electricity market: Residential solar PV adoption, electricity demand and prices, Energy Policy 122 (2018) 36 – 44 (2018).
- [19] I. Pérez-Arriaga, A. Bharatkuma, A framework for redesigning distribution network use of system charges under high penetration of distributed energy resources: new principles for new problems, Tech. rep., MIT CEEPR (2014).

- [20] F. Heymann, V. Miranda, F. J. Soares, P. Duenas, I. P. Arriaga, R. Prata, Orchestrating incentive designs to reduce adverse system-level effects of large-scale EV/PV adoption – the case of Portugal, Applied Energy 256 (2019) 113931 (2019).
- [21] G. Cardoso, M. Stadler, M. Bozchalui, R. Sharma, C. Marnay, A. Barbosa-Póvoa, P. Ferrão, Optimal investment and scheduling of distributed energy resources with uncertainty in electric vehicle driving schedules, Energy 64 (2014) 17 – 30 (2014).
- [22] D. Issicaba, M. A. da Rosa, F. O. Resende, B. Santos, J. A. P. Lopes, Long-term impact evaluation of advanced under frequency load shedding schemes on distribution systems with DG islanded operation, IEEE Transactions on Smart Grid 10 (1) (2019) 238–247 (Jan 2019).
- [23] R. Billington, R. N. Allan, Reliability Evaluation of Power Systems, 2nd Edition, Plenum, New York, USA, 1996 (1996).
- [24] M. E. Baran, F. F. Wu, Optimal capacitor placement on radial distribution systems, IEEE Transactions on Power Delivery 4 (1) (1989) 725–734 (1989).
- [25] K.-Y. Liu, W. Sheng, Y. Liu, X. Meng, Y. Liu, Optimal sitting and sizing of DGs in distribution system considering time sequence characteristics of loads and DGs, International Journal of Electrical Power & Energy Systems 69 (2015) 430 – 440 (2015).
- [26] M. Deru et al., U.S. Department of Energy Commercial Reference Building Models of the National Building Stock, Tech. rep., NREL (February 2011).
- [27] S. Wilcox, W. Marion, Users Manual for TMY3 Data Sets, Tech. rep., NREL (May 2008).
- [28] G. Cardoso, T. Brouhard, N. DeForest, D. Wang, M. Heleno, L. Kotzur, Battery aging in multi-energy microgrid design using mixed integer linear programming, Applied Energy 231 (2018) 1059 – 1069 (2018).